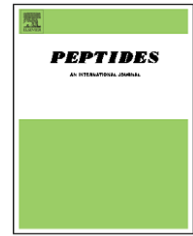ELSEVIER

Since January 2020 Elsevier has created a COVID-19 resource centre with free information in English and Mandarin on the novel coronavirus COVID-19. The COVID-19 resource centre is hosted on Elsevier Connect, the company's public news and information website.

# Peptides containing membrane-interacting motifs inhibit herpes simplex virus type 1 infectivity

Stefania Galdiero [a,b,c], Annarita Falanga [d], Mariateresa Vitiello [d],
Marina D'Isanto [d], Marco Cantisani [a,c], Aikaterini Kampanaraki [d],
Ettore Benedetti [a,b,c], Helena Browne [e], Massimiliano Galdiero [d,*]

[a] Department of Biological Sciences, Division of Biostructures, University of Naples "Federico II", Via Mezzocannone 16, 80134 Naples, Italy
[b] Centro Interuniversitario di Ricerca sui Peptidi Bioattivi, University of Naples "Federico II", Via Mezzocannone 16, 80134 Naples, Italy
[c] Istituto di Biostrutture e Bioimmagini, CNR, Via Mezzocannone 16, 80134 Naples, Italy
[d] Department of Experimental Medicine, II University of Naples, Via De Crecchio 7, 80138 Naples, Italy
[e] Division of Virology, Department of Pathology, University of Cambridge, Cambridge, UK

## ARTICLE INFO

## ABSTRACT

Herpes simplex virus (HSV) membrane fusion represents an attractive target for anti-HSV therapy. To investigate the structural basis of HSV membrane fusion and identify new targets for inhibition, we have investigated the different membranotropic domains of HSV-1 gH envelope glycoprotein. We observed that fusion peptides when added exogenously are able to inhibit viral fusion likely by intercalating with viral fusion peptides upon adopting functional structure in membranes. Interestingly, peptides analogous to the predicted HSV-1 gH loop region inhibited viral plaque formation more significantly. Their inhibitory effect appears to be a consequence of their ability to partition into membranes and aggregate within them. Circular dichroism spectra showed that peptides self-associate in aqueous and lipidic solutions, therefore the inhibition of viral entry may occur via peptides association with their counterpart on wild-type gH. The antiviral activity of HSV-1 peptides tested provides an attractive basis for the development of new fusion peptide inhibitors corresponding to regions outside the fusion protein heptad repeat regions.

© 2008 Elsevier Inc. All rights reserved.

## 1. Introduction

Herpes simplex virus type 1 (HSV-1) is a member of the α-herpesvirus subfamily and requires four membrane glycoproteins to mediate fusion, namely glycoprotein D (gD), glycoprotein B (gB), and the glycoprotein H and L complex (gH/L) are essential for fusion. HSV-1 mutants lacking one of those four glycoproteins are not infectious and their replication is blocked at membrane fusion [41,47].

Three of these glycoproteins are membrane spanning (gB, gD and gH), whereas gL is a soluble glycoprotein expressed at the virion and cell surface only in a heterodimer with gH. Besides, HSV-1 gH is not trafficked to the cell surface in the absence of gL [24].

The most complex and least understood stage in HSV-1 entry into mammalian cells is the fusion of the virion envelope with the cellular membrane. It has been extensively documented that the aforementioned set of distinct glycoproteins (gD, gB, gH/L) is necessary and sufficient for membrane fusion [36,52], following a stable binding of the virus to the cell [41,48].

Since gD does not have the characteristics of a fusion protein, it is assumed that the central fusion machinery

involves gB and the heterodimer gH/L. In fact, it has been described that interactions of gD with one of its receptors cause conformational changes in the N-terminal region of gD [2,28] that enable activation of the fusogenic process, which, according to the model proposed by Subramanian and Geragthy [51], is carried out, through a hemifusion intermediate, by the sequential activity of gH and gB.

Mainly two different classes of viral fusion proteins have been described on the bases of their common post-fusion structural motifs.

The Class I prototype (identified in orthomyxoviruses, paramyxoviruses, retroviruses, filoviruses and coronaviruses) [9,53,58,60,61], forms homotrimers that are cleaved proteolitically into a surface subunit and a transmembrane subunit anchored to the viral membrane. This fusion protein is extended to a rod-like structure in response to an activating trigger. A hydrophobic α-helix fusion peptide at the N-terminus of the transmembrane subunit is exposed and able to penetrate into the membrane of the apposing cell. A second conformational change brings together two heptad repeats (HR1 and HR2) located downstream of the fusion peptide, to form a coiled-coil structure resulting in a stable hairpin conformation. Activated proteins of this Class share the common 6-helix bundle, which is the functional unit that causes the folding back of the fusion protein upon itself and leads to the close contacts between the viral and cellular membranes in order to allow lipid mixing [44].

Class II proteins (flaviviruses and alphaviruses) [30,34,42], besides having a fusion peptide in an internal location, do not form coiled-coils and contain predominantly β-strand secondary structure. These glycoprotein are generally associated with a second protein as a heterodimer and activation is represented by the cleavage of the accessory protein leading to an irreversible rearrangement of the fusion protein into a trimer which protrude from the viral envelope allowing the penetration of the internal fusion peptide into the cell membrane. Again a foldback movement brings the two membranes enough close to start merging [25,26].

In contrast, HSV-1 needs the cooperation of four glycoproteins to gain access into the target cell, and gB and gH are the most likely candidates to be the fusion executors. Recent advances on the structural features of the HSV glycoproteins indicate that herpesviruses may use a somehow intermediate mechanism where its components may alone or in combination share characteristics of both Class I and Class II fusion proteins.

The recently solved crystal structure of HSV-1 gB reveals a trimeric ectodomain made up of five distinct domains in each monomer. The rod-shaped trimer is organized around a central helical core reminiscent of Class I fusion proteins [15,22], but gB fails to completely fall in this category since it is not proteolitically cleaved in two subunits therefore is lacking an N-terminal fusion peptide [40]. In particular, an α-helical coiled-coil core relates gB to Class I viral fusion proteins, while two extended β hairpins with hydrophobic tips, homologous to fusion peptides in VSV G, relate gB to Class II fusion proteins [22], therefore, a third class has been hypothesized [54].

Like gB, gH is conserved among the Herpesviridae family, and resembles viral fusion glycoproteins, having an internal putative fusion peptide [18] and two HR regions able to adopt a coiled-coil conformation [15].

Several domains likely to be important for membrane fusion have been identified in the gH ectodomain [13,17,18] and in the C-terminal region of the protein. For example, certain mutations in the transmembrane (TM) region and cytoplasmic tail affect fusion [1,21,57], as do mutations in the region preceding the TM [12]. The gH pre-transmembrane region itself has been proved to be involved in fusion interacting intimately with lipid membranes [14].

Several aspects of how gB and/or gH are activated by gD binding to cell receptors, and how they cooperate to direct fusion remain to be elucidated, but several of the structural/functional motifs present in different viral fusion glycoproteins have already been established as drug development targets [7].

For example, analogs of the orthomyxovirus, paramyxovirus, and HIV fusion peptides [27,43,45] block viral infection, presumably by forming inactive heteroaggregates. A second target for viral inhibition has proved to be the region forming coiled-coils through heptad repeat domains. It is generally accepted that fusion progresses by formation of an intermediate, a ''prehairpin'' conformation, that places the N-terminal fusion peptide near or in the target cell membrane, exposing the HR1 and HR2 regions [8]. In this intermediate, both HR are vulnerable to binding by synthetic peptides, which can thus inhibit viral infection by preventing formation of the fusogenic trimer-of-hairpins. HR2 peptides (Enfuvirtide), are potent inhibitors of HIV-1, active at low nanomolar concentration [32,56]. A competitive interaction with the HR1 domain and prevention of the 6-helix bundle conformation has been proposed as the mechanism of inhibition [4]. It was recently found that a peptide corresponding to the C-proximal region of α-1-antitrypsin, designated VIRIP, inhibits a wide variety of HIV-1 strains, by interacting with the gp41 fusion peptide and preventing its insertion into the target cell membrane. These studies indicate that the fusion peptide domain is an attractive drug target [37].

To date, studies examining peptide fusion inhibitors of herpesviruses have mainly focused on the analysis of peptides analogous to the HR regions of the putative fusion proteins gH and gB.

Synthetic peptides modeled on coiled coils region of BoHV-1 [38] and HCMV [31] have been described as inhibiting viral infection of susceptible cells. In HSV-1 both gH and gB have been found to possess HR regions [15,19], but only peptides from gH HR regions have been shown to inhibit fusion with a mechanism similar to what happens in HCMV fusion inhibition, since the most powerful peptides are the ones modeled on the HR1 at the N-terminus, which, nevertheless, need higher concentration to inhibit infectivity in respect to other viral systems [15].

Although the gH HR peptides appear to be inhibiting HSV-1 entry, development of other peptide fusion inhibitors, based on non-HR regions of the viral fusion protein has yet to be explored.

We previously reported that using a physio-chemical algorithm, the Wimley–White interfacial hydrophobicity scale in combination with other structural data we could predict regions involved in membrane interactions during the entry and fusion process [13].

| Table 1 – Peptide sequences | |
| --- | --- |
| Peptides | Sequence |
| gH220–262 | TWLATRGLLRSPGRYVYFSP-SASTWPVGIWTTGELVLGCDAAL |
| gH381–420 | RLTGLLATSGFAFVNAAHAN-GAVCLSDLLGFLAHSRALAG |
| gH493–537 | AAHLIDALYAEFLGGRVLTTPVVH-RALFYASAVLRQPFLAGVPSA |
| gH493–512 | AAHLIDALYAEFLGGRVLTT |
| gH626–644 | GLASTLTRWAHYNALIRAF |

In the present study, we have extended our previous work [13] and analyzed the infectivity inhibitory potential of the four regions, found to be able to induce membrane fusion (gH220–262, gH381–420, gH493–537, gH626–644). These regions, spanning the entire gH sequence, may play an important role in viral fusion protein:target cell membrane interactions and may therefore represent possible targets for therapeutic interference.

## 2. Methodology

### 2.1. Materials

Fluorenylmethoxycarbonyl (Fmoc) protected amino acids were purchased from INBIOS (Pozzuoli, NA, Italy), NovaSyn TGA resin from Nova Biochem (Darmstadt, Germany). The reagents (piperidine, pyridine) for the solid-phase peptide synthesis were purchased from Fluka (Sigma–Aldrich, Milano, Italy), trifluoroacetic acid (TFA) and acetic anhydride were from Applied Biosystem (Foster City, CA, USA). $H_2O$, DMF and $CH_3CN$ were supplied by LAB-SCAN (Dublin, Ireland). Acicloguanosine (ACV) was purchased from Sigma–Aldrich.

### 2.2. Bioinformatic analysis

The gH sequence used was taken from SWISS-Prot database, with accession number P08356. Hydropathy plots were obtained with Tmpred (ExPaSy, Swiss Institute of Bioinformatics) and Membrane Protein eXplorer (MpeX, Stephen White laboratory, http://blanco.biomol.uci.edu/mpex) as previously reported [13]. Secondary structure predictions were performed using Jpred software [6].

### 2.3. Peptide synthesis

Peptides were synthesized using standard solid-phase-9-fluorenylmethoxycarbonyl (Fmoc) method, on a PSSM8 multi-specific peptide synthesizer (Shimadzu Corporation Biotechnology Instruments Department, Kyoto, Japan), as previously reported [13]. Peptide sequences are reported in Table 1.

### 2.4. Liposome preparation

Large unilamellar vesicles (LUV) consisting of PC/Chol (1:1), and when necessary containing Rho-PE and NBD-PE, were prepared according to the extrusion method of Hope et al. [23] in 5 mM HEPES, 100 mM NaCl, pH 7.4. Lipids were dried from a chloroform solution with a nitrogen gas stream and lyophilized overnight. For fluorescence experiments, dry lipid films were suspended in buffer by vortex; then the lipid suspension was freeze–thawed six times and then extruded 20 times through polycarbonate membranes with 0.1 μm diameter pores to produce large unilamellar vesicles. Lipid concentrations of liposome suspensions were determined by phosphate analysis [10].

### 2.5. Lipid mixing assays

Membrane lipid mixing was monitored using the resonance energy transfer assay (RET) reported by Struck et al. [49]. The assay is based on the dilution of the NBD-PE (donor) and Rho-PE (acceptor). Dilution due to membrane mixing results in an increase in NBD-PE fluorescence.

Thus, we monitored the change in donor emission as aliquots of peptides were added to vesicles. Vesicles containing 0.6 mol% of each probe were mixed with unlabeled vesicles at a 1:4 ratio (final lipid concentration, 0.1 mM). Small volumes of peptides in dimethylsulfoxide (DMSO) were added; the final concentration of DMSO in the peptide solution was no higher than 2%. The NBD emission at 530 nm was followed with the excitation wavelength set at 465 nm. A cut off filter at 515 nm was used between the sample and the emission monochromator to avoid scattering interferences. The fluorescence scale was calibrated such that the zero level corresponded to the initial residual fluorescence of the labeled vesicles and the 100% value corresponding to complete mixing of all lipids in the system was set by the fluorescence intensity of vesicles upon the addition of Triton-X-100 (0.05%, v/v) at the same total lipid concentrations of the fusion assay. All fluorescence measurements were conducted in PC/Chol (1:1) LUV. Lipid mixing experiments were repeated at least three times and results were averaged. Control experiments were performed using scrambled peptides and DMSO.

### 2.6. Cells and virus

Vero cells were grown in Dulbecco's modified Eagle's medium (DMEM) supplemented with 10% fetal calf serum. HSV-1 carrying a LacZ gene driven by the CMV IE-1 promoter to express β-galactosidase was propagated as previously described [11].

### 2.7. Virus entry assays

Peptides were dissolved in DMEM without serum and used at a range of concentrations. All experiments were conducted in parallel with scrambled peptides and no-peptide controls. To assess the effect of peptides on inhibition of HSV infectivity, four different ways of treating cell monolayers were performed:

(a) For "virus pre-treatment", approximately $2 \times 10^4$ PFU of HSV-1 were incubated in the presence of different concentrations of peptides (10, 100, 250, 500 μM) for 45 min at 37 °C, then titrated on Vero cell monolayers.
(b) For "cell pre-treatment", Vero cells were incubated with peptides (10, 100, 250, 500 μM) for 30 min at 4 °C. Peptides

were removed, and cells were washed with phosphate-buffered saline (PBS) before being infected with serial dilutions of HSV-1 and incubated for 45 min at 37 °C.

(c) For "co-treatment", the cells were incubated with increasing concentrations of the peptides (10, 100, 250, 500 μM) in the presence of the viral inoculum for 45 min at 37 °C.

(d) For "post-treatment", Vero cells monolayers were challenged with HSV-1 for 45 min at 37 °C.

Different concentrations of peptides (10, 100, 250, 500 μM) were then added to the inoculum, followed by a further 30 min incubation at 37 °C.

For all treatments, nonpenetrated viruses were inactivated by citrate buffer at pH 3.0 after the 45 min incubation with cells at 37 °C. The cells were then incubated for 24 h at 37 °C in DMEM supplemented with CMC. Monolayers were fixed, stained with X-gal (5-bromo-4-chloro-3-indolyl-β-D-galacto-pyranoside) and plaque numbers were scored. Experiments were performed in triplicate and the percentage of inhibition was calculated with respect to no-peptide control experiments.

### 2.8. Toxicity

Peptide cytotoxicity was measured by a lactate dehydrogenase (LDH) assay which was carried out according to manufacturer's instructions using a cytotoxicity detection kit (Roche Diagnostic SpA., Milano, Italy).

### 2.9. Circular dichroism measurements

CD spectra were recorded using a Jasco J-715 spectropolarimeter in a 1.0 or 0.1 cm quartz cell at room temperature. Titration of peptides (20 μM) in various percentages of TFE were performed as well as titration as a function of peptide concentration in buffer, TFE20% and lipids. Solutions of peptides (5–20–50–100–200 μM) were prepared in buffer, in TFE 20% and in lysophosphatydilcholine (LC) SUVs. Peptide samples in lipids were prepared using the following protocol [20]: all peptides were first dissolved in TFE; immediately after preparation, the peptide solution was added to an equal volume of a chloroform solution containing the appropriate lipid concentration; solutions were dried with a nitrogen gas stream and lyophilized overnight; the dry samples were rehydrated with deionized water to yield a final lipid concentration of 0.9 mM. Small unilamellar vesicles (SUV) of lysophosphatydilcholine (LC) were prepared from MLVs by sonication. The spectra are an average of three consecutive scans from 260 to 195 nm, recorded with a band width of 3 nm, a time constant of 16 s and a scan rate of 10 nm/min. Spectra were recorded and corrected for the blank. Mean residues ellipticities (MRE) were calculated using the equation Obsd/$lcn$ where Obsd is the ellipticities measured in millidegrees, $l$ is the length of the cell in cm, $c$ is the peptide concentration in mol/l, and $n$ is the number of amino acid residues in the peptide. The percentage of helix was calculated from measurements of their mean residue ellipticity at 222 nm [3]. We used [[ϑ]222 values of 0 and −40.000 $(1 − 2.5/n)$ deg cm$^2$ dmol$^{-1}$ per amino acid residue for 0 and 100% helicity; $n$ is the number of amino acid residues.

### 2.10. Native gel electrophoresis

Isolated peptides (7.5 μl of a solution 1 mM in phosphate buffer, pH 7.3) and mixtures of peptides with 4 mM and 5 mM SDS were incubated at 25 °C for 5 min (final volume of 11 μl) and analyzed by Native gel electrophoresis. Gel electrophoresis was carried out for 2.5 h in gels consisting of 4% polyacrylamide for the stacking gel and 12% for the separating gel at a constant amperage of 30 mA using a Bio-Rad Mini-Protean cell. The gel was stained with Coomassie brilliant blue R-250.

## 3. Results

### 3.1. Bioinformatic analysis

We have previously used a computational approach to identify regions of gH that potentially interact with bilayer membranes (Wimley–White). Six regions of high interfacial hydrophobicity were identified using MpeX [55,59], four of them proved to be capable of inducing fusion of liposomes in vitro. In particular, peptides gH220–262, gH381–420, and gH626–644 were the most active and play a fundamental role in the fusion process. Peptide gH493–537 although not being very active alone was shown to have a cooperative fusogenic effect when used in combination with the other active peptides [13]. This peptide (gH493–537) corresponds to the region comprised between the two HR domains of gH, and a shorter sequence of its C-terminus, namely gH513–531, showed an increased ability to induce fusion of lipid vesicles [17]. The secondary structure prediction reveals that the region from residue 493 to 537 is composed of two helices separated by a kink at residue Pro513, thus the two helices may have a different function in the fusion mechanism. We thus decided to synthesize the sequence from 493 to 512 (Fig. 1), and to test it in fusion and inhibition experiments.

### 3.2. Lipid mixing assay

We have previously reported that peptides gH220–262, gH381–420, gH493–537 and gH626–644 of HSV-1 gH are able to induce fusion of unilamellar vesicles (LUV) composed of PC/Chol (1:1), as revealed by the probe dilution assay. A population of LUVs labeled with both NBD-PE and Rho-PE was mixed with a population of unlabeled LUVs and increasing amounts of peptides were added. Fusion between the labeled and unlabeled vesicles caused by the peptides results in dilution of the labeled lipids and therefore reduced energy transfer between NBD-PE and Rho-PE, visualized as an increase of NBD fluorescence. The dependence of the extent of lipid mixing on the peptide to lipid molar ratio was analyzed. The fusion experiment has been performed on the gH493–512 peptide in order to determine its ability to induce fusion. Increasing amounts of gH493–512 peptide were added to a fixed amount of vesicles and in order to compare the activity of the different peptides, the percentage of lipid mixing as a function of the peptide to lipid molar ratio is reported in Fig. 2 for all the peptides.
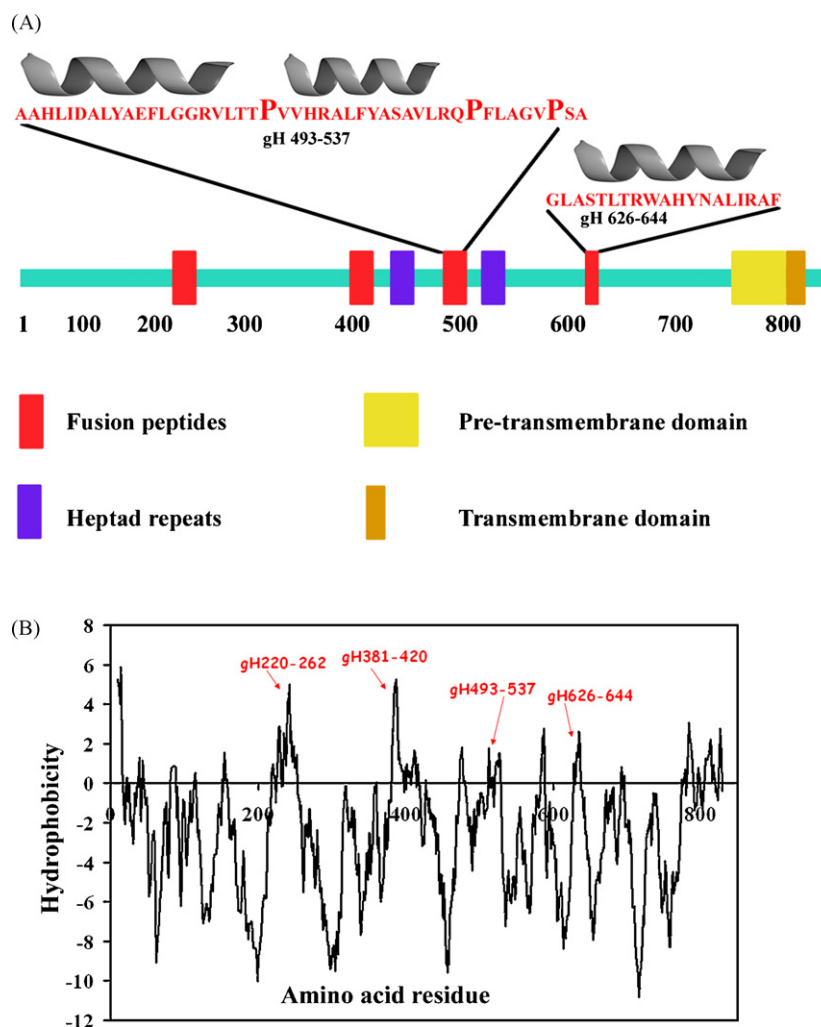
Fig. 1 – (A) HSV-1 gH protein diagram and secondary structure prevision and (B) hydrophobicity plot.

Our data demonstrate that gH493–512, representing the shorter N-terminal analog of the peptide comprised in between the HR domains of gH, is unable to induce fusion at least in the experimental conditions used in this assay.

### 3.3. Effect of fusion peptides of gH on virus infectivity

The five peptides (gH220–262, gH381–420, gH493–537, gH493–512 and gH626–644), corresponding to the domains with high scores of the Wimley and White hydrophobicity, which previously were shown to interact with biological membranes, were screened for their ability to inhibit plaque formation (Table 1).

To verify that these peptides did not exert toxic effect on Vero cells, monolayers were exposed to different concentrations (100, 250 and 500 $\mu$M) of each peptide for 24 h, and cell viability was assayed by an LDH assay. No statistical difference was observed between the viability of control (untreated) cells and that of cells exposed to the peptides (data not shown).

To test whether these peptides from gH could affect HSV infectivity, we inoculated HSV-1 onto Vero cells at 37 °C in the presence or absence of each peptide under a range of different conditions as described in Section 2.1. These results are shown in Fig. 3.

In a dose-dependent inhibition assay of HSV entry, peptides gH220–262 and gH381–420 showed non-significant activity up to 500 $\mu$M. On the contrary, peptides gH493–537 and gH626–644 were able to inhibit HSV entry with approximately 50–60% of inhibition at 250 $\mu$M and 60–70% at 500 $\mu$M. The shorter peptide gH493–512, corresponding only to the N-terminus of gH493–537, was able to inhibit HSV entry even more effectively, resulting in approximately 60% inhibition at 250 $\mu$M and a 90% of inhibition at 500 $\mu$M (Fig. 3A). To obtain a 50% plaque reduction, it was necessary only 160 $\mu$M of gH493–512 and 60 $\mu$M of gH626–644. The peptide gH626–644 was the most difficult to dissolve and thus inhibition at 500 $\mu$M was strongly dependent on the preparation of the sample; these data were further supported by CD data reported in the following paragraph, demonstrating that the peptide oligomerises already at 50 $\mu$M.

Further experiments were, therefore, carried out to identify the step in the entry process which was inhibited by the four peptides. We choose a peptide concentration of 250 $\mu$M that gave a significant inhibition in the previous experiment
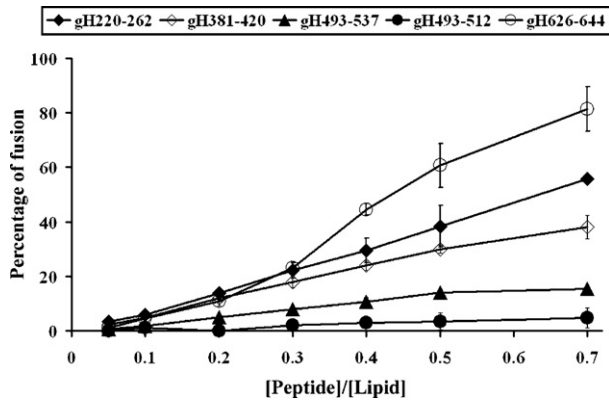
Fig. 2 – gH peptides induced fusion of unilammellar vesicles. Peptide-promoted membrane fusion of PC/Chol (1:1) LUV as determined by lipid mixing; peptide aliquots were added to 0.1 mM LUV, containing 0.6% NBD and 0.6% Rho. The increase in the fluorescence was measured 15 min after the addition of peptide aliquots; reduced Triton-X-100 (0.05%, v/v) was referred to as 100% of fusion. The dose dependence of lipid mixing is reported.

(Fig. 3A) with the co-exposure treatment without strong bias due to the solubility of peptides and compared the effect of three other different methods of exposure of the cells and/or virus to peptide (Fig. 3B). gH220–262 and gH381–420 were not effective in any of the experiments. gH493–537 and its shorter version gH493–512 are able to inhibit infectivity only when present during the period of virus attachment-entry into cells, in fact they were not active in the post-exposure treatment, in which cells were infected with HSV-1 for 45 min and only afterwards the peptide was added to the inoculum and they were not active in cell-preexposure experiments. On the contrary the peptide gH626–644 is more active in co-exposure and cell pre-exposure experiments than in virus pre-incubation experiments.

A scrambled version of gH493–512 (the most active peptide in all experiments), was included as control and failed to inhibit HSV-1 infectivity under similar experimental conditions (Fig. 3).

The two active peptides, gH493–512 and gH626–644 ranked in order of potency, seem to behave with a different mechanism of action, since the latter is also able to inhibit virus infectivity when treating cell before the viral challenge.

To determine the specificity of the inhibitory effect of peptides derived from HSV-1 gH we tested the two most effective inhibitors of HSV-1 infection (gH493–512 and gH626–644) for their ability to inhibit the infectivity of an unrelated enveloped virus (parainfluenza-2 virus, a member of the Paramyxoviridae). In Fig. 3, panel C is shows that none of these peptides exerted any significant effect on parainfluenzavirus-2 (PIV-2), thus supporting the view that the inhibition observed with HSV-1 is specific.

### 3.4. Secondary structure of synthetic peptides

Since the structural conformation of fusion peptides has been shown to relate to fusogenic activity, the secondary structure
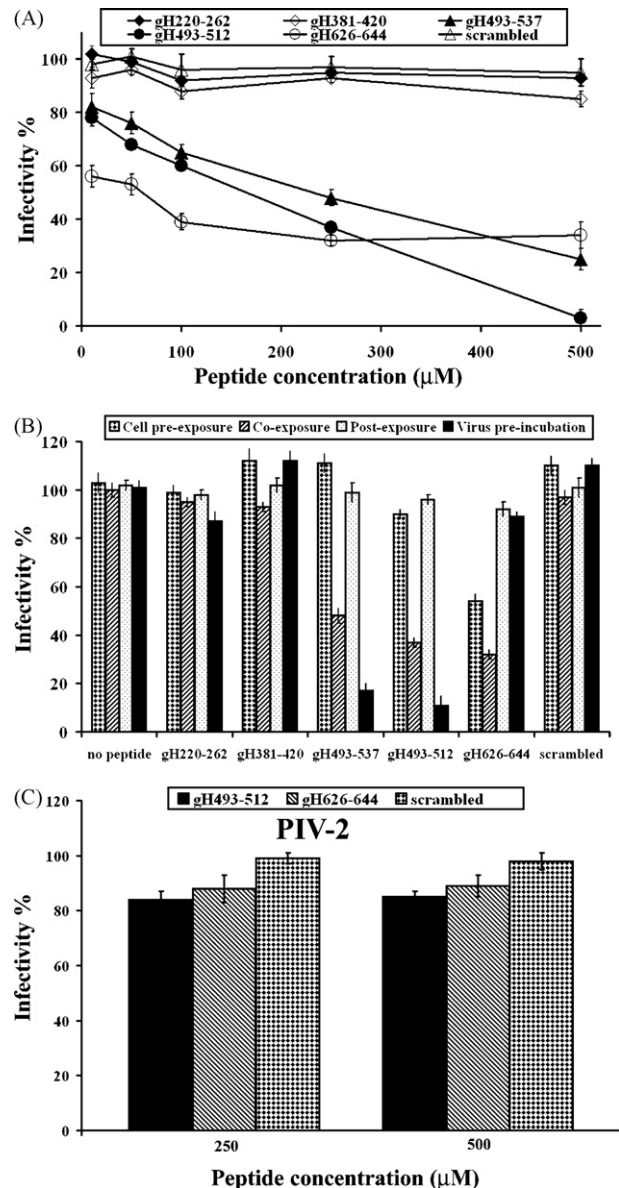


Fig. 3 – Inhibition of viral infectivity. (A) Vero cells were incubated with increasing concentrations of the peptides (10, 50, 100, 250, 500 μM) in the presence of the viral inoculum for 45 min at 37 °C. (B) Cells were exposed to active peptides at a concentration of 250 μM either prior to infection (cells pre-exposure), during attachment and entry (co-exposure), after virus penetration (post-exposure), or alternatively, the virus was pre-incubated with peptides for 1 h at 37 °C before addition to the cells (virus preincubation). (C) Cells were exposed to active peptides (gH493–512 and gH626–644) at a concentration of 250 and 500 μM and PIV-2 in the co-exposure mode. For all treatments, non-penetrated viruses were inactivated by low-pH citrate buffer after the 45 min incubation with cells at 37 °C. The cells were then, incubated for 48 h at 37 °C in DMEM supplemented with CMC and plaque numbers were scored. Experiments were performed in triplicate and the percentage of inhibition was calculated with respect to no-peptide control experiments. Error bars represent standard deviations.
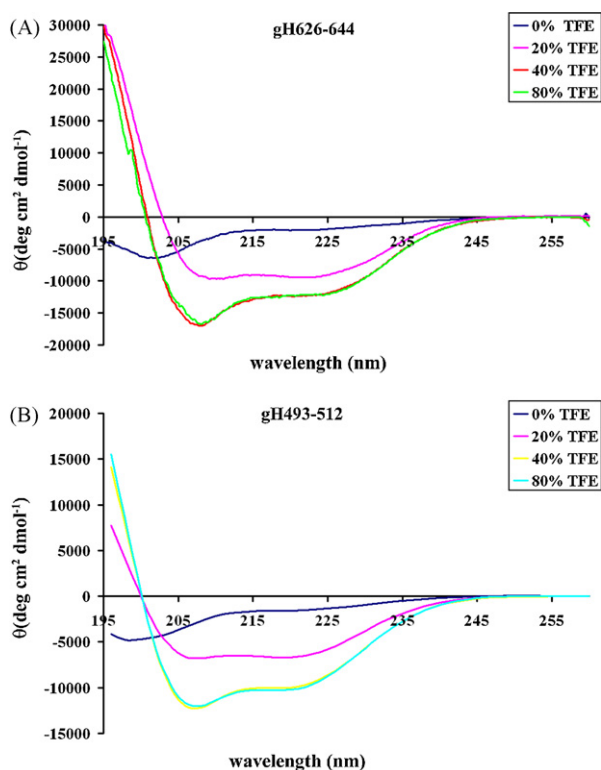
Fig. 4 – Secondary structure of gH peptides by CD spectroscopy. Circular dichroism spectra of gH626–644 (A) and gH493–512 (B) at different percentages of TFE.



Fig. 5 – Circular dichroism spectra of gH. Circular dichroism spectra of gH626–644 (A) and gH493–512 (B) at different peptide concentrations.

of peptides was determined by CD spectroscopy as measured in water, TFE and SUV. In all conditions tested, the spectra were not reliable below 195 nm because of light-scattering, and therefore are not shown. We reported only CD experiments performed on the two most active peptides in inhibition experiments, namely gH493–512 and gH626–644.

The CD spectrum in buffer solution indicated a random coil conformation for both peptides (Fig. 4). A decrease in peptide environmental polarity occurs when the peptide is transferred from water to membrane interfaces; the effect of polarity on peptide conformation can be studied using aqueous mixtures of TFE (Fig. 4). In the presence of 20% TFE, both peptides already showed two negative bands at about 208 and 222 nm, suggesting the adoption of an α-helical conformation; calculations of helix content according to Chakrabartty et al. [3] corresponded to a percentage of helix of 27% for peptide gH626–644 and of 19% for peptide gH493–512; increasing concentrations of TFE induced a further helical stabilization (approximately 35% for gH626–644 and 28% for gH493–512). These results suggest that both peptides contain a particular sequence of amino acids that in a non-polar environment can adopt an α-helical conformation.

CD spectroscopy was also utilized to test whether the two peptides gH493–512 and gH626–644 create oligomers in solution. Our data clearly demonstrate that both peptides adopt a random coil conformation in buffer solution and their CD spectra remained practically unaltered in the whole concentration range studied (5–200 μM) (data not shown).
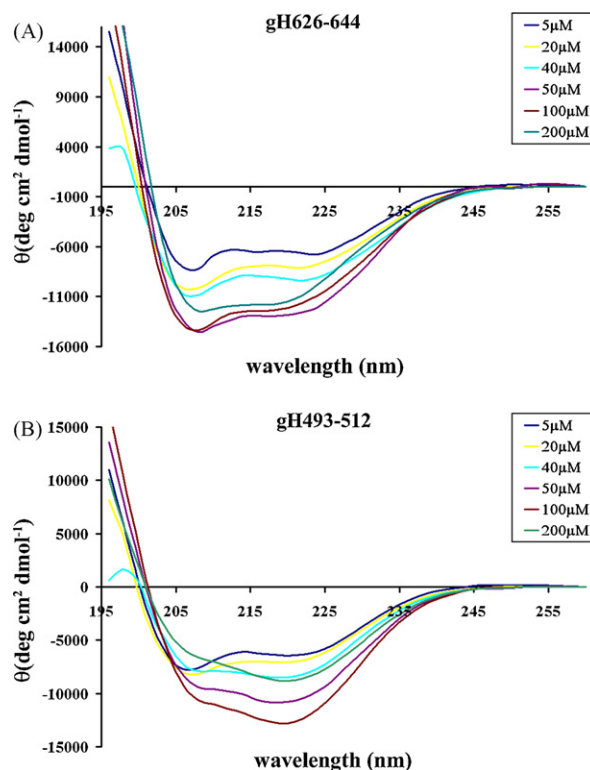
The titration of gH626–644 as a function of TFE (Fig. 4A), showed that already in the presence of 20% TFE, the peptide adopts an α-helical conformation. The ratio of the ellipticities at 222 and 208 nm can be utilized to distinguish between monomeric and oligomeric states of helices [33]; when the ratio $\theta222/\theta208$ equals about 0.8, the peptide is in its monomeric state, and when the ratio exceeds the value of 1.0 is in its oligomeric state. The data reveal that in presence of 20% TFE gH626–644 adopts an α-helical conformation with the monomer/oligomer equilibrium shifted toward the oligomeric state with a ratio $\theta222/\theta208$ of approximately 1.05, while at higher percentages of TFE the ratio decreases to 0.76 indicating a monomeric state. Lau et al. [29] have previously shown that TFE 50% disrupts the quaternary structure of α-helices, i.e. TFE is a denaturant of tertiary and quaternary structure stabilized by hydrophobic interactions. We thus assayed the secondary structure dependence from the concentration in a solution containing 20% TFE, a condition in which gH626–644 showed the presence of oligomeric species (Fig. 4A). In 20% TFE, the peptide gH626–644 revealed a characteristic α-helix spectrum, with an ellipticity strongly dependent on concentration, suggesting the formation of aggregates (Fig. 5A). We concluded, however, that the aggregates were molecular in size because centrifugation, which removes precipitated hydrophobic peptides from solution, had no effect on the spectra. Furthermore, a strong concentration dependence of the helicity would not be expected for macroscopic aggregates. From the ellipticity at 222 nm, we estimated helicities of about 19% at 5 μM and of about 36% for 50 μM, at higher concentra-

tion it starts to diminish and at 200 μM is approximately 31%. The data reveal values of $\theta222/\theta208$ always around 1 indicating that the peptide is always in its oligomeric state. The same analysis were performed on gH493–512. The titration of gH493–512 as a function of TFE (Fig. 4B), showed that in 20% TFE, the peptide adopts an α-helical conformation, with a percentage of helix of 19%; the ratio of the ellipticities at 222 and 208 nm reveals that at this percentage of TFE, the peptide is in its oligomeric state with a ratio $\theta222/\theta208$ of approximately 1.00, while at higher percentages of TFE the ratio is approximately 0.80 indicating a monomeric state. In 20% TFE (Fig. 5B), also the peptide gH493–512 revealed a characteristic α-helix spectrum, with an ellipticity strongly dependent on concentration, suggesting the formation of aggregates. As for gH626–644, we believe that the aggregates were molecular in size because centrifugation had no effect on the spectra. From the ellipticity at 222 nm, we estimated helicities of about 18% at 5 μM and of about 35% for 100 μM, at 200 μM decreases to approximately 25%. A similar behaviour with a sudden fall in molecular ellipticity was previously observed for aggregating peptides [5]. Moreover, the two peptides show a similar tendency to associate and produce molecular aggregates of helices but the critical concentration differs for the two peptides, in particular the maximum ellipticity was observed at 50 μM for gH626–644 and at 100 μM for gH493–512, indicating a greater tendency of gH626–644 to aggregate (Fig. 5).

### 3.5. The oligomeric state of the peptides with NATIVE-PAGE electrophoresis

The tendency of the peptides gH626–644 and gH493–512 to oligomerize was further explored in NATIVE-PAGE (Fig. 6) using isolated peptides and peptides with 4 mM and 5 mM SDS. SDS has been used previously to determine the aggregation state of membrane proteins [46] and fusion peptides [27]. The analysis of the band pattern of each peptide in absence or presence of SDS enabled us to better understand the oligomerization profile. The NATIVE-PAGE without SDS and with 4 mM and 5 mM SDS reveals that both peptides
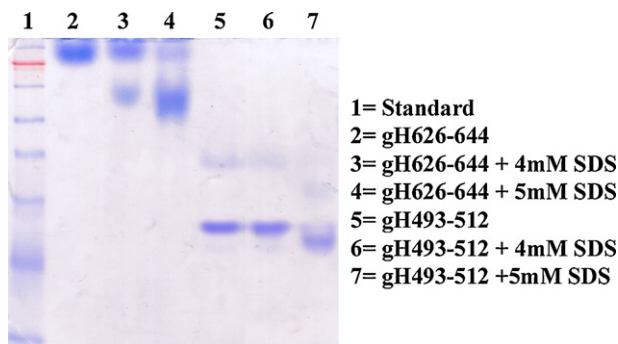


Fig. 6 – Native gel electrophoresis of gH peptides. Lane 1: molecular weight standard (188 kDa; 98 kDa; 62 kDa; 49 kDa; 38 kDa; 28 kDa; 15 kDa; 4 kDa); lane 2: gH626–644; lane 3: gH626–644 treated with 4 mM SDS; lane 4: gH626–644 treated with 5 mM SDS; lane 5: gH493–512; lane 6: gH493–512 treated with 4 mM SDS; lane 7: gH493–512 treated with 5 mM SDS.

oligomerize but gH626–644 forms higher order oligomers compared to gH493–512 (Fig. 6). In absence of SDS gH626–644 (lane 2) presents one band at very high molecular weight approximately between 49 and 62 kDa and gH493–512 (lane 5) present one main band between 15 and 28 kDa and a small band at higher molecular weight. The presence of SDS 5 mM (lanes 4 and 7) is enough to induce partially the dissociation of oligomers for both peptides. Our results indicate that both peptides have a tendency to oligomerize but gH626–644 gives higher order oligomers, thus confirming the CD data.

## 4. Discussion

Hydropathy analysis based on the hydrophobicity-at-interface scale proposed by Wimley and White [59] enabled us to detect six domains of HSV gH that may be involved in the interaction of the virus envelope and host cell membranes. We have previously demonstrated that only sequences gH220–262, gH381–420, gH493–537 and gH626–644 of HSV-1 gH are able to induce rapid membrane fusion and to act in a synergistic way. The four peptides of gH are surely involved in the process of a close interaction with the target membrane thereby promoting the formation of fusion intermediates, and in particular gH626–644 is the most active in fusion.

HSV-1 gH is directly involved in the fusion process, presumably in the formation of the hemifusion intermediate. The mechanism whereby gH mediates hemifusion needs to take into account the possibility that this large glycoprotein contains several membrane-interacting segments having a high tendency to locate at the interface between the viral and the target membranes, as previously reported for Sendai virus [16] and HIV [35,50]. gH presents a fusion peptide exposed on a fusion loop rather than at the N-terminal side, but it seems that several different fusogenic domains are needed to execute complete fusion.

Moreover, it has been recently demonstrated that the HR1 and HR2 regions of HSV-1 gH can indeed form a complex typical of other type 1 fusion proteins and they function as inhibitors of infection [13].

We recently proved that the domain between the two heptad repeats (HR1 and HR2) corresponding to the peptide gH493–537 has a membrane-interacting ability, binds and interacts with phospholipid model membranes and although being poorly fusogenic, when used alone, it has a synergic activity with other segments of gH. Its ability to induce membrane fusion parallel recent results reported on HIV gp41 loop domain [39]. The peptide gH493–537 and principally its shorter analog gH493–512 are also able to inhibit the entry of HSV-1. Interestingly, it was recently reported [17] that deletion of the C-terminus of gH493–537, from a 513 to aa 531, and its replacement with heterologous fusion peptides in a sense or antisense direction, decreases infection to less than 10% relative to wt-gH and almost abolished cell–cell fusion. A synthetic peptide corresponding to gH513–531 is able to induce fusion of lipid vesicles more effectively than gH493–512, even though the results of fusion percentages cannot be precisely compared due to different experimental conditions; and is also able to increase virus infection and cell–cell fusion. The present study, which has investigated sequences gH493–537

and gH493–512, indicate that gH493–537 is able to induce liposome fusion only in combination with the other three fusogenic domains, while both gH493–537 and gH493–512 alone are unable to significantly induce liposome fusion. The present results together with available data on gH513–531 [17], seem to support the hypothesis that only the C-terminus of this domain is involved in fusion; on the contrary the sequence gH493–512 is unable to induce liposome fusion but strongly inhibits virus infection. The analysis of the secondary structure prediction of protein gH indicates that the domain gH493–537 may adopt an α-helical structure with a kink at the proline 513; moreover there are other two proline residues (proline 529 and 535) toward the C-terminus, which are usually present in sequences interacting with membranes, further supporting the hypothesis that the C terminus may be involved in membrane fusion.

gH626–644 and gH493–512 did not precipitate or otherwise form macroscopic aggregates in presence of membranes at least at the concentrations assayed in CD studies (5–200 μM). The strong dependence of secondary structure on concentration is indicative of the formation of molecular aggregates in membranes and was also confirmed by Page experiments. In inhibition experiments also a concentration of 500 μM was tested and we observed controversial results for gH626–644 probably indicating a precipitation of the peptide at this concentration.

Peptides gH626–644 and gH493–512 showed the strongest inhibitory effect observed for peptides modeled on HSV-1 fusion glycoproteins to date. Their inhibitory effect appears conditioned by their ability to partition into membranes and aggregate within them. Since the peptides self-associate in aqueous and lipidic solutions, it is possible that they bind to their counterparts in the HSV-1 gH fusion protein, thus suggesting that the inhibition of viral entry may occur via peptides association with their counterpart on wild-type gH. The main difference between the active peptides analyzed, is that gH626–644 may more intimately interact with the host cell membrane, therefore its ability to partially inhibit viral entry, when cells are treated first, is dependent on the possibility that the virus will find a modified cell membrane still exhibiting on its surface the peptide. On the other hand the loop domain gH493–512 is more powerful in the virus preincubation experiment, showing a direct activity of the peptide on the viral glycoprotein.

Moreover, it is interesting to note that gH626–644 does not have any activity in the virus preincubation experiment, where approximately $2 \times 10^4$ PFU of HSV-1 are incubated in the presence of different concentrations of peptides, thus, indicating that this high hydrophobic region is probably hidden and not available to interactions with peptides in gH pre-fusogenic conformation.

Several structural conformational changes induced by a complex series of protein–protein and protein–phospholipid interactions occur in fusion proteins. However, little is known about how these conformational changes drive membrane apposition and how they overcome the energy barrier for membrane fusion. It is now evident that several domains are essential for membrane fusion and thus peptides involved in the fusion mechanism may interfere with the intramolecular interactions between the several domains and result in the inhibition of HSV-1 entry. Further studies are required to define the inhibitory mechanism of these HSV-1 peptides, probably due to different degrees of interaction with membranes and with their protein counterparts. We hypothesise that gH493–512 and gH626–644 may sterically hinder their relative domain, either in a pre-fusogenic or in an intermediate conformation, preventing a complete and functional interaction between gH and the membrane to fuse.

The inhibition of membrane fusion represents an attractive target for drug design and although further studies are needed to better define the exact mechanism of inhibition by these peptides and the specific nature or location of their interactions with viral targets, the data shown in this work suggest that the domain comprised between the two heptad repeats domains play a significant role in membrane fusion and provide an alternative approach to the development of viral peptide inhibitors outside of the HR regions.

## REFERENCES

[1] Browne H, Bell S, Minson T, Wilson DW. An endoplasmic reticulum-retained herpes simplex virus glycoprotein H is absent from secreted virions: evidence for reenvelopment during egress. J Virol 1996;70:4311–6.

[2] Carfi A, Willis SH, Whitbeck JC, Krummenacher C, Cohen GH, Eisenberg RJ, Wiley DC. Herpes simplex virus glycoprotein D bound to the human receptor HveA. Mol Cell 2001;8:169–79.

[3] Chakrabartty A, Kortemme T, Baldwin RL. Helix propensities of the amino acids measured in alanine-based peptides without helix-stabilizing side-chain interactions. Protein Sci 1994;3:843–52.

[4] Chan DC, Kim PS. HIV entry and its inhibition. Cell 1998;93:681–4.

[5] Chetal P, Chauhan VS, Sahal D. A meccano set approach of joining trpzip a water soluble beta-hairpin peptide with a didehydrophenylalanine containing hydrophobic helical peptide. J Peptide Res 2005;65:475–84.

[6] Cuff JA, Barton GJ. Application of enhanced multiple sequence alignment profiles to improve protein secondary structure prediction. Proteins Struct Funct Genet 2000;40:502–11.

[7] Dimitrov DS. Virus entry: molecular mechanisms and biomedical applications. Nat Rev Microbiol 2004;2: 109–22.

[8] Eckert DM, Kim PS. Mechanism of viral membrane fusion and its inhibition. Annu Rev Biochem 2001;70:777–810.

[9] Fass D, Harrison SC, Kim PS. Retrovirus envelope domain at 1.7 angstrom resolution. Nat Struct Biol 1996;3:465–9.

[10] Fiske CH, Subbarow Y. The colorimetric determination of phosphorus. J Biol Chem 1925;66:374–89.

[11] Forrester A, Farrell H, Wilkinson G, Kaye J, Davis-Poynter N, Minson T. Construction and properties of a mutant of herpes simplex virus type 1 with glycoprotein H coding sequences deleted. J Virol 1992;66:341–8.

[12] Galdiero M, Whiteley A, Bruun B, Bell S, Minson T, Browne H. Site-directed and linker insertion mutagenesis of herpes simplex virus type 1 glycoprotein H. J Virol 1997;71:2163–70.

[13] Galdiero S, Falanga A, Vitiello M, Browne H, Pedone C, Galdiero M. Fusogenic domains in herpes simplex virus type 1 glycoprotein H. J Biol Chem 2005;31:28632–43.

[14] Galdiero S, Falanga A, Vitiello M, D'Isanto M, Collins C, Orrei V, Browne H, Pedone C, Galdiero M. Evidence for a role of the membrane-proximal region of herpes simplex virus

Type 1 glycoprotein H in membrane fusion and virus inhibition. Chembiochem 2007;8:885–95.

[15] Galdiero S, Vitiello M, D'Isanto M, Falanga A, Collins C, Raieta K, Pedone C, Browne H, Galdiero M. Analysis of synthetic peptides from heptad-repeat domains of herpes simplex virus type 1 glycoproteins H and B. J Gen Virol 2006;87:1085–97.

[16] Ghosh JK, Shai Y. A peptide derived from a conserved domain of Sendai virus fusion protein inhibits virus-cell fusion. A plausible mode of action. J Biol Chem 1998;273:7252–9.

[17] Gianni T, Fato R, Bergamini C, Lenaz G, Campadelli-Fiume G. Hydrophobic alpha-helices 1 and 2 of herpes simplex virus gH interact with lipids, and their mimetic peptides enhance virus infection and fusion. J Virol 2006;80:8190–8.

[18] Gianni T, Martelli PL, Casadio R, Campadelli-Fiume G. The ectodomain of herpes simplex virus glycoprotein H contains a membrane alpha-helix with attributes of an internal fusion peptide, positionally conserved in the herpesviridae family. J Virol 2005;79:2931–40.

[19] Gianni T, Menotti L, Campadelli-Fiume G. A heptad repeat in herpes simplex virus 1 gH, located downstream of the alpha-helix with attributes of a fusion peptide, is critical for virus entry and fusion. J Virol 2005;79:7042–9.

[20] Han X, Steinhauer DA, Wharton SA, Tamm LK. Interaction of mutant influenza virus hemagglutinin fusion peptides with lipid bilayers: probing the role of hydrophobic residue size in the central region of the fusion peptide. Biochemistry 1999;38:15052–9.

[21] Harman A, Browne H, Minson T. The transmembrane domain and cytoplasmic tail of herpes simplex virus type 1 glycoprotein H play a role in membrane fusion. J Virol 2002;76:10708–16.

[22] Heldwein EE, Lou H, Bender FC, Cohen GH, Eisenberg RJ, Harrison SC. Crystal structure of glycoprotein B from herpes simplex virus 1. Science 2006;313:217–20.

[23] Hope MJ, Bally MB, Webb G, Cullis PR. Production of large unilamellar vesicles by a rapid extrusion procedure: characterization of size, trapped volume and ability to maintain a membrane potential. Biochim Biophys Acta 1985;812:55–65.

[24] Hutchinson L, Browne H, Wargent V, Davis-Poynter N, Primorac S, Goldsmith K, Minson AC, Johnson DC. A novel herpes simplex virus glycoprotein, gL, forms a complex with glycoprotein H (gH) and affects normal folding and surface expression of gH. J Virol 1992;66:2240–50.

[25] Jardetzky TS, Lamb RA. Virology: a class act. Nature 2004;427:307–8.

[26] Kielian M. Class II virus membrane fusion proteins. Virology 2006;344:38–47.

[27] Kliger Y, Aharoni A, Rapaport D, Jones P, Blumenthal R, Shai Y. Fusion peptides derived from the HIV type 1 glycoprotein 41 associate within phospholipid membranes and inhibit cell–cell Fusion. Structure-function study. J Biol Chem 1997;272:13496–505.

[28] Krummenacher C, Supekar VM, Whitbeck JC, Lazear E, Connolly SA, Eisenberg RJ, Cohen GH, Wiley DC, Carfi A. Structure of unliganded HSV gD reveals a mechanism for receptor-mediated activation of virus entry. EMBO J 2005;24:4144–53.

[29] Lau SY, Taneja AK, Hodges RS. Synthesis of a model protein of defined secondary and quaternary structure. Effect of chain length on the stabilization and formation of two-stranded alpha-helical coiled-coils. J Biol Chem 1984;259:13253–61.

[30] Lescar J, Roussel A, Wien MW, Navaza J, Fuller SD, Wengler G, Wengler G, Rey FA. The fusion glycoprotein shell of Semliki Forest virus: an icosahedral assembly primed for fusogenic activation at endosomal pH. Cell 2001;105:137–48.

[31] Lopper M, Compton T. Coiled-coil domains in glycoproteins B and H are involved in human cytomegalovirus membrane fusion. J Virol 2004;78:8333–41.

[32] Matthews T, Salgo M, Greenberg M, Chung J, DeMasi R, Bolognesi D. Enfuvirtide: the first therapy to inhibit the entry of HIV-1 into host CD4 lymphocytes. Nat Rev Drug Discov 2004;3:215–25.

[33] Meng FG, Zeng X, Hong YK, Zhou HM. Dissociation and unfolding of GCN4 leucine zipper in the presence of sodium dodecyl sulfate. Biochimie 2001;83:953–6.

[34] Modis Y, Ogata S, Clements D, Harrison SC. A ligand-binding pocket in the dengue virus envelope glycoprotein. Proc Natl Acad Sci USA 2003;100:6986–91.

[35] Moreno MR, Pascual R, Villalain J. Identification of membrane-active regions of the HIV-1 envelope glycoprotein gp41 using a 15-mer gp41-peptide scan. Biochim Biophys Acta 2004;1661:97–105.

[36] Muggeridge MI. Characterization of cell–cell fusion mediated by herpes simplex virus 2 glycoproteins gB, gD, gH and gL in transfected cells. Gen Virol 2000;81:2017–27.

[37] Munch J, Standker L, Adermann K, Schulz A, Schindler M, Chinnadurai R, Pohlmann S, Chaipan C, Biet T, Peters T, Meyer B, Wilhelm D, Lu H, Jing W, Jiang S, Forssmann WG, Kirchhoff F. Discovery and optimization of a natural HIV-1 entry inhibitor targeting the gp41 fusion peptide. Cell 2007;129:263–75.

[38] Okazaki K, Kida H. A synthetic peptide from a heptad repeat region of herpesvirus glycoprotein B inhibits virus replication. J Gen Virol 2004;85:2131–7.

[39] Pascual R, Moreno MR, Villalaín J. A peptide pertaining to the loop segment of human immunodeficiency virus gp41 binds and interacts with model biomembranes: implications for the fusion mechanism. J Virol 2005;79:5142–52.

[40] Pereira L. Function of glycoprotein B homologues of the family herpesviridae. Infect Agents Dis 1994;3:9–28.

[41] Reske A, Pollara G, Krummenacher C, Chain BM, Katz DR. Understanding HSV-1 entry glycoproteins. Rev Med Virol 2007;17:205–15.

[42] Rey FA, Heinz FX, Mandl C, Kunz C, Harrison SC. The envelope glycoprotein from tick-borne encephalitis virus at 2 A resolution. Nature 1995;375:291–8.

[43] Richardson CD, Scheid A, Choppin PW. Specific inhibition of paramyxovirus and myxovirus replication by oligopeptides with amino acid sequences similar to those at the N-termini of the F1 or HA2 viral polypeptides. Virology 1980;105:205–22.

[44] Schibli DJ, Weissenhorn W. Class I and Class II viral fusion protein structures reveal similar principles in membrane fusion. Mol Membr Biol 2004;21:361–71.

[45] Silburn KA, McPhee DA, Maerz AL, Poumbourios P, Whittaker RG, Kirkpatrick A, Reilly WG, Manthey MK, Curtain CC. Efficacy of fusion peptide homologs in blocking cell lysis and HIV-induced fusion. AIDS Res Hum Retrovirus 1998;14:385–92.

[46] Simmerman HK, Kobayashi YM, Autry JM, Jones LR. A leucine zipper stabilizes the pentameric membrane domain of phospholamban and forms a coiled-coil pore structure. J Biol Chem 1996;271:5941–6.

[47] Spear PG. Herpes simplex virus: receptors and ligands for cell entry. Cell Microbiol 2004;6:401–10.

[48] Spear PG, Manoj S, Yoon M, Jogger CR, Zago A, Myscofski D. Different receptors binding to distinct interfaces on herpes simplex virus gD can trigger events leading to cell fusion and viral entry. Virology 2006;344:17–24.

[49] Struck DK, Hoekstra D, Pagano RE. Use of resonance energy transfer to monitor membrane fusion. Biochemistry 1981;20:4093–9.

[50] Suarez T, Gallaher WR, Agirre A, Goni FM, Nieva JL. Membrane interface-interacting sequences within the ectodomain of the human immunodeficiency virus type 1 envelope glycoprotein: putative role during viral fusion. J Virol 2000;74:8038–47.

[51] Subramanian RP, Geraghty RJ. Herpes simplex virus type 1 mediates fusion through a hemifusion intermediate by sequential activity of glycoproteins D, H, L, and B. Proc Natl Acad Sci USA 2007;104:2903–8.

[52] Turner A, Bruun B, Minson T, Browne H. Glycoproteins gB, gD, and gHgL of herpes simplex virus type 1 are necessary and sufficient to mediate membrane fusion in a Cos cell transfection system. J Virol 1998;72:873–5.

[53] Weissenhorn W, Carfi A, Lee KH, Skehel JJ, Wiley DC. Crystal structure of the Ebola virus membrane fusion subunit, GP2, from the envelope glycoprotein ectodomain. Mol Cell 1998;2:605–16.

[54] Weissenhorn W, Hinz A, Gaudin Y. Virus membrane fusion. FEBS Lett 2007;581:2150–5.

[55] White SH, Wimley WC. Membrane protein folding and stability: physical principles. Annu Rev Biophys Biomol Struct 1999;28:319–65.

[56] Wild C, Oas T, McDanal C, Bolognesi D, Matthews T. A synthetic peptide inhibitor of human immunodeficiency virus replication: correlation between solution structure and viral inhibition. Proc Natl Acad Sci USA 1992;89: 10537–41.

[57] Wilson DW, Davis-Poynter N, Minson AC. Mutations in the cytoplasmic tail of herpes simplex virus glycoprotein H suppress cell fusion by a syncytial strain. J Virol 1994;68:6985–93.

[58] Wilson IA, Skehel JJ, Wiley DC. Structure of the haemagglutinin membrane glycoprotein of influenza virus at 3 A resolution. Nature 1981;289:366–73.

[59] Wimley WC, White SH. Experimentally determined hydrophobicity scale for proteins at membrane interfaces. Nat Struct Biol 1996;3:842–8.

[60] Xu Y, Liu Y, Lou Z, Qin L, Li X, Bai Z, Pang H, Tien P, Gao GF, Rao Z. Structural basis for coronavirus-mediated membrane fusion. Crystal structure of mouse hepatitis virus spike protein fusion core. J Biol Chem 2004;279:30514–22.

[61] Yin HS, Wen X, Paterson RG, Lamb RA, Jardetzky TS. Structure of the parainfluenza virus 5 F protein in its metastable, prefusion conformation. Nature 2006;439:38–44.